Lyle, M., Koizumi, I., Richter, C., and Moore, T.C., Jr. (Eds.), 2000
Proceedings of the Ocean Drilling Program, Scientific Results, Vol. 167

7. STABLE ISOTOPE STRATIGRAPHY AND PALEOCEANOGRAPHY OF THE LAST 170 K.Y.: SITE 1014, TANNER BASIN, CALIFORNIA[1]

I.L. Hendy[2] and J.P. Kennett[2]

ABSTRACT

Late Quaternary oxygen ($\delta^{18}O$) and carbon ($\delta^{13}C$) isotopic records for the benthic foraminifer *Uvigerina* and the planktonic foraminifer *Globigerina bulloides* are presented for the upper 20 meters composite depth sediment sequence of Ocean Drilling Program Site 1014, Tanner Basin, in the outer California Borderland province. The benthic oxygen isotopic record documents a continuous >160-k.y. sequence from marine isotope Stage (MIS) 6 to the present day. The record closely resembles other late Quaternary North Pacific benthic isotope records, as well as the well-dated deep-sea sequence (SPECMAP), and thus provides a detailed chronologic framework.

Site 1014 provides a useful record of the California response to climate change as it enters the southern California Borderland. Sedimentation rates are relatively constant and high (~11.5 cm $k.y.^{-1}$). The planktonic foraminiferal record is well preserved except during marine isotope Substages 5b and 5d, when normally high *G. bulloides* abundance is strongly diminished as a result of dissolution. The planktonic oxygen isotopic shift of ~3‰ between the last glacial maximum and the Holocene suggests a surface water temperature shift of <7°C, similar to estimates from Hole 893A (Leg 146) to the north. Unlike Santa Barbara Basin, *G. bulloides* $\delta^{18}O$ values during the last interglacial (MIS 5) at Site 1014 were significantly higher than during the Holocene. In particular, marine isotope Substage 5e (Eemian) was ~0.8‰ higher. This is unlikely to reflect a cooler Eemian but is instead the result of preferential dissolution of thin-shelled (low $\delta^{18}O$) specimens during this interval. In this mid-depth basin, a large benthic $\delta^{18}O$ shift during Termination I suggests dramatic temperature and salinity changes in response to switches in the source of North Pacific Intermediate Water.

Although $\delta^{13}C$ values of the planktonic foraminifer *G. bulloides* are in disequilibria with seawater and hence interpretations are limited, the *G. bulloides* record exhibits several negative $\delta^{13}C$ excursions found at other sites in the region (Sites 1017 and 893). This indicates a response of *G. bulloides* $\delta^{13}C$ to regional surface water processes along the southern California margin. A general increase in benthic carbon isotopic values (–1.75‰ to –0.75‰) in Tanner Basin during the last 200 k.y. is overprinted with smaller fluctuations correlated with climate change. The coolest intervals during the last glacial maximum (MISs 2 and 4) exhibit lower benthic $\delta^{13}C$ values, which correlate with global $\delta^{13}C$ shifts. The opposite relationship is exhibited during the last interglacial before 85 ka, when lower benthic $\delta^{13}C$ values are associated with warmer intervals (marine isotope Substages 5c and 5e) of the last interglacial. These time intervals were also marked by decreased intermediate water ventilation. Increased dissolution and organic accumulation during Substages 5b and 5d are anticorrelated with the benthic $\delta^{13}C$ record. These results suggest that a delicate balance in intermediate water $\delta^{13}C$ has existed between the relative influences of global $\delta^{13}C$ and regional ventilation changes at the 1165-m water depth of Site 1014.

INTRODUCTION

Information on the late Neogene paleoclimatic evolution of the California Borderland is well expressed in the sedimentary record because of the region's high sensitivity to climate change and its known high biological productivity (Emery, 1960; Kennett and Ingram, 1995; Behl and Kennett, 1996; Mortyn and Thunell, 1997). Tanner Basin is located ~150 km west of San Diego (south of Santa Barbara Basin) within the outer band of the California Borderland basins (Fig. 1). This contribution describes the late Quaternary oxygen and carbon isotope stratigraphy and paleoceanography of Tanner Basin, Site 1014 (32°50.046′N; 119°58.879′W) from a depth of 1177 m. The site, being relatively close to the North American continent, experiences high sedimentation rates, which enhance the stratigraphic resolution of paleoclimatic reconstructions. Thus, the site was drilled with the express purpose of examining the late Neogene paleoceanographic evolution of the California Current system in the outer Borderland province.

Tanner Basin is primarily influenced by the southerly flowing California Current (Fig. 1) (Reid et al., 1958). The inner edge of the California Current flows along the outer periphery of the Borderland (except during spring) and turns toward the coast near San Diego. The average surface flow in the central portion of the Borderland is the northerly flowing southern California Countercurrent (Fig. 1). The northern Channel Islands substantially block this flow, and much of the current is diverted to the west, where it merges with the California Current (Lynn and Simpson, 1987). This results in the formation of a counterclockwise-flowing gyre in the southern California bight (except during spring). The net flow beneath these two currents is the northward-flowing California Undercurrent (Lynn and Simpson, 1987; Reid et al., 1958).

The strength and location of these currents are determined by ocean-atmosphere interactions over a broad area of the North Pacific Ocean. Predominant northerly winds associated with the seasonal migration of the North Pacific high pressure cell in spring and summer cause strong flow of the California Current to the south; when the northerly winds weaken in winter, the undercurrent strengthens (Pisias, 1978). This creates two other circulation forces within the southern California margin: wind stress or Ekman transport, which is strongest near Point Conception, and geostrophic flow (pressure gradient) produced by a higher sea level resulting from nearshore warm water in the San Diego region. During spring and summer, the two forces oppose each other, resulting in cyclonic circulation in the re-

[1]Lyle, M., Koizumi, I., Richter, C., and Moore, T.C., Jr. (Eds.), 2000. *Proc. ODP, Sci. Results,* 167: College Station TX (Ocean Drilling Program).

[2]Department of Geological Sciences and Marine Science Institute, University of California, Santa Barbara CA 93106, USA. Correspondence author: hendy@magic.geol.ucsb.edu

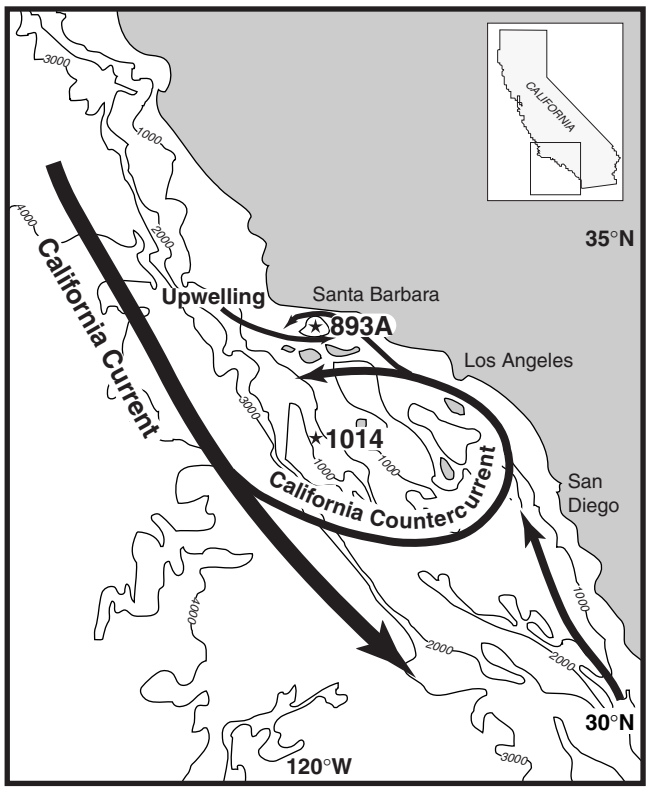

Figure 1. Location of Site 1014, Tanner Basin, on the southern California margin overlain by the major surface currents of the region. Hole 893A (Santa Barbara Basin) is also indicated. Bathymetry is in meters.

gion (Winant and Dorman, 1997). Thus, regional sensitivity of sea-surface temperatures (SSTs) to climate change is produced by tight coupling between the atmospheric and surface ocean over the North Pacific.

The southern California margin is composed of the California Borderland and continental slope, viewed as an extension of highly irregular shelf morphology ranging seaward of the true continental slope (Gorsline and Teng, 1989). At depth, the North Pacific Intermediate Water, with sources in the deep Pacific, flows across sills into the basins of the southern California Borderland. Therefore, bottom waters within these basins reflect intermediate water at the depth of these sills and are further altered by internal processes within the basins (Emery, 1954). Recent studies have suggested that intermediate waters in the North Pacific underwent large changes during the late Quaternary and appear to play a role in climate change (Kennett and Ingram, 1995; Behl and Kennett, 1996; van Geen et al., 1996). As a result, it is important to evaluate and understand changes that occurred in intermediate waters in the context of climate change. Ocean Drilling Program (ODP) Leg 167 has provided deep-sea cores from a number of southern California basins. Benthic records from these sites should broaden our understanding of the role of mid-ocean depths in climate change. Because Site 1014 lies near the limit of the Pacific Intermediate Water, it is possible to investigate depths of ventilation switches in the North Pacific during the Quaternary.

METHODS AND MATERIALS

Sampling of Site 1014 for stable isotopic investigations was conducted at moderately high stratigraphic resolution to allow the development of a useful chronological framework for investigators studying the uppermost sections of this site. Four holes were drilled from 1164 to 1167 m, with sequences ranging from 19.5 to 404.4 m recovered from the site. Core recovery was excellent and exceeded 100% because of gas expansion as the sediments contained biogenic methane. Detailed comparisons between magnetic susceptibility, gamma-ray attenuation porosity evaluator density, and high-resolution color reflectance allowed splicing between cores from the four holes and demonstrated complete recovery of the sequence down to 160 meters below seafloor (Lyle, Koizumi, Richter, et al., 1997).

Two-centimeter samples of 10 cm^3 volume were taken from Site 1014 at 5-cm intervals for the upper 20 meters composite depth (mcd). The raw samples were disaggregated in warm water, washed over a 63-μm sieve, and oven dried at 50°C. The remaining coarse fraction was split, with one-half to be used for stable isotope analysis and the other half kept intact for archival purposes. Benthic foraminiferal stable isotope analyses were conducted on 194 samples. Approximately eight to 10 clean, entire *Uvigerina* spp. specimens were picked for benthic isotope analysis at 10-cm intervals in the upper 20 mcd of the site (Table 1). *Uvigerina* is a benthic foraminiferal taxon frequently utilized for isotopic stratigraphic studies of marine sediments. It precipitates its test close to oxygen isotopic equilibrium (Shackleton, 1974) and thus provides reliable $\delta^{18}O$ records. Isotope analysis of the planktonic foraminiferal species *Globigerina bulloides* was undertaken at 5-cm intervals in the upper 14.5 mcd interval and at 10-cm intervals from 14.5 to 20.0 mcd on 284 samples (Table 1). The $\delta^{18}O$ of *G. bulloides* represents surface water conditions since this species lives in the near-surface (0–20 m) (Pak and Kennett, 1997) and tolerates a wide temperature range (6°–26°C) (Thunell and Sautter, 1992).

Specimens picked for isotopic analysis were cleaned ultrasonically in reagent-grade methanol then dried and roasted under vacuum at 350°C for 1 hr to remove organic contaminants. The samples were reacted in orthophosphoric acid at 90°C with an on-line automated carbonate CO_2 preparation device, and evolved CO_2 was analyzed using a Finningan/MAT 251 light stable isotope mass spectrometer. Instrument precision is 0.09‰ or better for $\delta^{18}O$ and $\delta^{13}C$. All isotopic data are expressed using standard δ notation in per mil (‰) relative to Peedee belemnite (PDB) carbonate standard. Isotopic analysis is related to PDB through repeated analysis of NBS-19, with values following Coplen (1996) of –2.2 for $\delta^{18}O$ and 1.95 for $\delta^{13}C$.

STRATIGRAPHY AND CHRONOLOGY

The recovered sequence at Site 1014 provides a continuous Pliocene to Quaternary record of hemipelagic sedimentation underlain by a poorly dated upper Miocene sequence. The upper Quaternary sequence at Site 1014 consists of hemipelagic clay interbedded (every 30 to 120 cm) with nannofossil ooze, with foraminifers throughout (Lyle, Koizumi, Richter, et al., 1997). Bedding contacts are gradational, and the sediments are slightly bioturbated. An initial well-constrained biostratigraphy and chronology are provided by a combination of calcareous nannofossil, planktonic foraminifer, and radiolarian datums for the upper Pliocene and Quaternary (Lyle, Koizumi, Richter, et al., 1997). Further chronology is also provided by the paleomagnetic record through the identification of the Brunhes/Matuyama boundary and the Jaramillo Subchronozone (Lyle, Koizumi, Richter, et al., 1997).

A more detailed chronology is given using the well-established global changes in the relative abundance of stable oxygen isotopes (SPECMAP) (Martinson et al., 1987). The benthic oxygen isotope record mainly represents the global removal and storage of the light oxygen isotope (^{16}O) from seawater during cool intervals through major ice-sheet accumulation (and thus sea-level change). A $\delta^{18}O$ record obtained from the benthic foraminiferal species *Uvigerina* for the upper 20 mcd of Site 1014 exhibits the familiar sawtooth pattern of the

Table 1. Benthic and planktonic foraminiferal oxygen and carbon isotopic data from Site 1014.

Core, section, interval (cm)	Depth (mcd)	Age (ka)	*G. bulloides* ($\delta^{18}O$)	*G. bulloides* ($\delta^{13}C$)	*Uvigerina* ($\delta^{18}O$)	*Uvigerina* ($\delta^{13}C$)
167-1014D-						
1H-1, 0-2	0.00	0.00	–0.113	–1.235		
1H-1, 5-7	0.05	0.33	0.440	–0.175		
1H-1, 10-12	0.10	0.65	0.633	–0.379		
1H-1, 15-17	0.15	0.98	0.535	–0.415	3.025	–0.798
1H-1, 20-22	0.20	1.30	0.451	–0.673		
1H-1, 25-27	0.25	1.63	0.859	–0.711	2.807	–0.810
1H-1, 30-32	0.30	1.95	0.195	–0.647		
1H-1, 35-37	0.35	2.28	0.266	–0.885	2.572	–1.017
1H-1, 40-42	0.40	2.61	–0.265	–0.639		
1H-1, 45-47	0.45	2.93	–0.387	–0.596	2.708	–0.885
1H-1, 50-52	0.50	3.26	–0.200	–1.016		
1H-1, 55-57	0.55	3.58	–0.364	–0.530	2.693	–0.938
1H-1, 60-62	0.60	3.91	–0.486	–0.844		
1H-1, 65-67	0.65	4.23	–0.463	–0.638	2.879	–0.875
1H-1, 70-72	0.70	4.56	0.015	–0.832		
1H-1, 75-77	0.75	4.89	0.321	–0.621	3.040	–1.067
1H-2, 0-2	0.85	5.54	–0.320	–0.905		
1H-2, 5-7	0.90	5.86	–0.145	–0.511	3.053	–1.012
1H-2, 10-12	0.95	6.19	0.120	–0.723		
1H-2, 15-17	1.00	6.51	0.250	–0.693	3.354	–0.955
1H-2, 20-22	1.05	6.84	0.168	–0.776		
1H-2, 25-27	1.10	7.16	–0.100	–0.656	3.414	–1.158
1H-2, 30-32	1.15	7.49	0.174	–0.789		
1H-2, 35-37	1.20	7.82	0.326	–0.589	3.358	–0.991
1H-2, 40-42	1.25	8.14	0.244	–0.925		
1H-2, 45-47	1.30	8.47	0.242	–0.782	3.265	–1.026
1H-2, 50-52	1.35	8.79	0.341	–0.813		
1H-2, 55-57	1.40	9.12	0.299	–0.759	3.566	–1.193
1H-2, 60-62	1.45	9.44	0.367	–0.870		
1H-2, 65-67	1.50	9.77	0.701	–0.873	3.415	–1.183
1H-2, 70-72	1.55	10.10	0.422	–1.000		
1H-2, 75-77	1.60	10.42	0.657	–1.020	3.703	–1.233
1H-3, 0-2	1.70	11.07	0.783	–1.104		
1H-3, 5-7	1.75	11.40	0.656	–0.978	3.753	–1.194
1H-3, 10-12	1.80	11.72	0.710	–1.190		
1H-3, 15-17	1.85	12.05	0.608	–1.218	3.701	–1.202
1H-3, 20-22	1.90	12.88	1.753	–0.578		
1H-3, 25-27	1.95	13.71	2.167	–0.564	3.858	–1.287
1H-3, 30-32	2.00	14.54	2.074	–0.569	3.632	–1.062
1H-3, 35-37	2.05	15.36	2.383	–0.545	4.084	–1.411
1H-3, 40-42	2.10	16.19	2.530	–0.388	4.277	–1.203
1H-3, 45-47	2.15	17.02	2.623	–0.520	4.260	–1.331
1H-3, 50-52	2.20	17.85	2.601	–0.486		
1H-3, 55-57	2.25	18.24	2.467	–0.413	4.439	–1.201
1H-3, 60-62	2.30	18.63	2.391	–0.395		
1H-3, 65-67	2.35	19.02	2.341	–0.561	4.249	–1.459
1H-3, 70-72	2.40	19.42	2.204	–0.463		
1H-3, 75-77	2.45	19.81	2.308	–0.461	4.325	–1.433
1H-3, 80-82	2.50	20.20	2.063	–0.403		
1H-3, 85-87	2.55	20.59	2.201	–0.344	4.474	–1.453
1H-3, 90-92	2.60	20.98	2.427	–0.427		
1H-3, 95-97	2.65	21.37	2.120	–0.701	4.277	–1.420
1H-3, 100-102	2.70	21.76	2.162	–0.434		
1H-3, 105-107	2.75	22.15	2.361	–0.301	4.386	–1.321
1H-3, 110-112	2.80	22.55	2.167	–0.563		
1H-3, 115-117	2.85	22.94	2.256	–0.444	4.454	–1.348
1H-3, 120-122	2.90	23.33	2.028	–0.551		
1H-3, 125-127	2.95	23.72	2.263	–0.571	4.343	–1.198
1H-3, 130-132	3.00	24.11	2.257	–0.446		
1H-3, 135-137	3.05	24.42	2.243	–0.646	4.26	–1.379
1H-4, 0-2	3.15	25.04	2.341	–0.421		
1H-4, 5-7	3.20	25.35	1.959	–0.640	4.324	–1.201
1H-4, 10-12	3.25	25.65	2.264	–0.334		
1H-4, 15-17	3.30	25.96	2.049	–0.587	4.234	–1.164
1H-4, 20-22	3.35	26.27	2.194	–0.884		
1H-4, 25-27	3.40	26.58	2.173	–0.696	4.253	–1.131
1H-4, 30-32	3.45	26.89	2.229	–0.374		
1H-4, 35-37	3.50	27.20	2.054	–0.595	4.316	–1.136
1H-4, 40-42	3.55	27.51	2.218	–0.763		
1H-4, 45-47	3.60	27.82	2.037	–0.737	4.268	–1.138
1H-4, 50-52	3.65	28.13	2.124	–0.624		
1H-4, 55-57	3.70	28.43	1.996	–0.738	4.328	–1.242
1H-4, 60-62	3.75	28.74	2.075	–0.790		
1H-4, 65-67	3.80	29.05	1.834	–0.661	4.237	–1.184
1H-4, 70-72	3.85	29.36	1.848	–0.647		
1H-4, 75-77	3.90	29.67	1.744	–0.686	4.261	–1.223
1H-4, 80-82	3.95	29.98	2.023	–0.440		
1H-4, 85-87	4.00	30.29	2.085	–0.550	4.160	–1.313
1H-4, 90-92	4.05	30.60	2.155	–0.578		
1H-4, 95-97	4.10	30.91	2.278	–0.363	4.194	–1.021
1H-4, 100-102	4.15	31.21	2.164	–0.264		
1H-4, 105-107	4.20	31.52	1.981	–0.407	4.316	–0.934
1H-4, 110-112	4.25	31.83	2.076	–0.320		
1H-4, 115-117	4.30	32.14	2.176	–0.275	4.095	–1.096
1H-4, 120-122	4.35	32.45	1.910	–0.384		
1H-4, 125-127	4.40	32.76	2.100	–0.322	4.105	–1.104
1H-4, 130-132	4.45	33.07	2.006	–0.302		
1H-4, 135-137	4.50	33.38	2.127	–0.187	4.32	–1.098

Table 1 (continued).

Core, section, interval (cm)	Depth (mcd)	Age (ka)	*G. bulloides* ($\delta^{18}O$)	*G. bulloides* ($\delta^{13}C$)	*Uvigerina* ($\delta^{18}O$)	*Uvigerina* ($\delta^{13}C$)
1H-4, 140-142	4.55	33.69	1.911	–0.253		
1H-4, 145-147	4.60	34.00	1.729	–0.388		
1H-5, 0-2	4.60	34.00	1.735	–0.533	4.055	–1.286
1H-5, 5-7	4.65	34.30	2.073	–0.268	4.053	–1.194
1H-5, 10-12	4.70	34.61	1.918	–0.238		
1H-5, 15-17	4.75	34.92	1.747	–0.257	4.138	–1.220
1H-5, 20-22	4.80	35.23	1.548	–0.463		
1H-5, 25-27	4.85	35.54	1.773	–0.457	3.938	–1.132
1H-5, 30-32	4.90	35.85	2.027	–0.312		
1H-5, 35-37	4.95	36.16	2.146	–0.382	4.039	–1.209
1H-5, 40-42	5.00	36.47	1.966	–0.333		
167-1014B-						
2H-2, 14-16	5.11	37.15	2.036	–0.115	4.086	–0.981
2H-2, 20-22	5.17	37.52	1.528	–0.232		
2H-2, 25-27	5.22	37.83	1.419	–0.396	4.054	–1.091
2H-2, 30-32	5.27	38.13	1.426	–0.134		
2H-2, 35-37	5.32	38.44	1.878	0.238	4.109	–0.971
2H-2, 40-42	5.37	38.75	1.935	0.093		
2H-2, 45-47	5.42	39.06	1.674	–0.056	4.068	–1.019
2H-2, 50-52	5.47	39.37	2.116	–0.334		
2H-2, 55-57	5.52	39.68	1.607	–0.504	4.046	–0.955
2H-2, 60-62	5.57	39.99	2.061	–0.371		
2H-2, 65-67	5.62	40.30	1.813	–0.482	4.044	–0.979
2H-2, 70-72	5.67	40.61	2.019	–0.230		
2H-2, 75-77	5.72	40.91	1.472	–0.571	4.105	–0.990
2H-2, 80-82	5.77	41.22	1.830	–0.451		
2H-2, 85-87	5.82	41.53	1.262	–0.589	4.036	–0.901
2H-2, 90-92	5.87	41.84	1.460	–0.595		
2H-2, 95-97	5.92	42.15	1.666	–0.424	4.020	–0.976
2H-2, 100-102	5.97	42.46	2.040	–0.321		
2H-2, 105-107	6.02	42.77	1.784	–0.584	3.920	–0.880
2H-2, 110-112	6.07	43.08	1.572	–0.493		
2H-2, 115-117	6.12	43.39	1.500	–0.688	4.057	–0.882
2H-2, 120-122	6.17	43.69	1.721	–0.302		
2H-2, 125-127	6.22	44.16	1.567	–0.415	3.839	–1.096
2H-2, 130-132	6.27	44.86	1.867	–0.251		
2H-2, 135-137	6.32	45.57	1.528	–0.336	4.076	–0.971
2H-2, 140-142	6.37	46.27	1.914	–0.421		
2H-2, 145-147	6.42	46.97	1.566	–0.355	3.966	–1.106
2H-3, 0-2	6.47	47.68	1.838	–0.357		
2H-3, 5-7	6.52	48.38	1.651	–0.466	4.197	–1.161
2H-3 10-12	6.57	49.08	1.689	–0.530		
2H-3, 15-17	6.62	49.79	1.738	–0.377	3.932	–0.905
2H-3, 20-22	6.67	50.40	1.999	–0.364		
2H-3, 25-27	6.72	50.88	2.198	–0.230	3.869	–1.070
2H-3, 30-32	6.77	51.35	1.992	–0.254		
2H-3, 35-37	6.82	51.83	1.827	–0.464	4.003	–1.023
2H-3, 40-42	6.87	52.31	1.934	–0.332		
2H-3, 45-47	6.92	52.78	1.540	–0.376	4.031	–1.277
2H-3, 50-52	6.97	53.26	1.825	–0.494		
2H-3, 55-57	7.02	53.74	1.468	–0.605	4.026	–1.215
2H-3, 60-62	7.07	54.21	1.723	–0.539		
2H-3, 65-67	7.12	54.69	1.559	–0.705	3.993	–1.229
2H-3, 70-72	7.17	55.16	1.829	–0.567		
2H-3, 75-77	7.22	55.73	1.811	–0.452	3.806	–1.491
2H-3, 80-82	7.27	56.43	2.271	–0.395		
2H-3, 85-87	7.32	57.13	2.315	–0.399	3.91	–1.185
2H-3, 90-92	7.37	57.84	2.166	–0.495		
2H-3, 95-97	7.42	58.54	2.023	–0.597	3.973	–1.353
2H-3, 100-102	7.47	59.15	2.278	–0.317		
2H-3, 105-107	7.52	59.61	2.096	–0.223	4.037	–1.274
2H-3, 110-112	7.57	60.08	2.402	–0.356		
2H-3, 115-117	7.62	60.55	2.455	–0.382	4.106	–1.102
2H-3, 120-122	7.67	61.01	2.506	–0.263		
2H-3, 125-127	7.72	61.48	2.095	–0.511	4.106	–1.198
2H-3, 130-132	7.77	61.94	2.172	–0.477		
2H-3, 135-137	7.82	62.41	2.098	–0.380	4.132	–1.117
2H-3, 140-142	7.87	62.88	2.090	–0.535		
2H-3, 145-147	7.92	63.34	2.229	–0.295	4.133	–1.178
2H-4, 0-2	7.97	63.81	2.175	–0.372		
2H-4, 5-7	8.02	64.37	1.922	–0.514		
2H-4, 5-7	8.02	64.37	2.252	–0.402	4.078	–1.328
2H-4, 10-12	8.07	65.07	2.242	–0.243		
2H-4, 15-17	8.12	65.77	2.268	–0.276	4.142	–1.254
2H-4, 20-22	8.17	66.47	2.081	–0.472		
2H-4, 25-27	8.22	67.18	2.181	–0.539	4.000	–1.259
2H-4, 30-32	8.27	67.88	2.134	–0.422		
2H-4, 35-37	8.32	68.58	2.271	–0.310	4.053	–1.309
2H-4, 40-42	8.37	69.28	2.338	–0.138		
2H-4, 45-47	8.42	69.98	1.862	–0.595	3.927	–1.284
2H-4, 50-52	8.47	70.68	1.958	–0.321		
2H-4, 55-57	8.52	71.38	1.637	–0.466	3.962	–1.270
2H-4, 65-67	8.62	72.79	1.552	–0.389	3.918	–1.254
2H-4, 75-77	8.72	74.01			3.745	–1.111
2H-4, 85-87	8.82	74.49			3.730	–1.264
2H-4, 90-92	8.87	74.74	1.927	–0.634		
2H-4, 95-97	8.92	74.98	1.815	–0.299	3.737	–1.251
2H-4, 100-102	8.97	75.22	1.649	–0.286		

Table 1 (continued).

Core, section, interval (cm)	Depth (mcd)	Age (ka)	*G. bulloides* ($\delta^{18}O$)	*G. bulloides* ($\delta^{13}C$)	*Uvigerina* ($\delta^{18}O$)	*Uvigerina* ($\delta^{13}C$)
2H-4, 105-107	9.02	75.46	1.949	–0.429	3.737	–1.036
2H-4, 110-112	9.07	75.71	1.430	0.047		
2H-4, 115-117	9.12	75.95	1.504	–0.054	3.625	–1.005
2H-4, 120-122	9.17	76.19	2.108	–0.072		
2H-4, 125-127	9.22	76.43	1.804	–0.405	3.696	–0.975
2H-4, 130-132	9.27	76.68	1.730	0.097	3.692	–0.907
2H-4, 140-142	9.37	77.16	1.734	0.076	3.630	–0.989
2H-5, 0-2	9.47	77.65	1.534	–0.528	3.458	–0.983
2H-5, 10-12	9.57	78.13	1.847	–0.592		
2H-5, 15-17	9.62	78.38	1.990	–0.442	3.439	–1.091
2H-5, 20-22	9.67	78.62	1.878	–0.622	3.394	–1.065
2H-5, 30-32	9.77	79.10	1.666	–0.366		
2H-5, 35-37	9.82	79.56			3.238	–1.084
2H-5, 45-47	9.92	81.12			3.311	–1.047
2H-5, 55-57	10.02	82.68			3.332	–0.951
2H-5, 60-62	10.07	83.46	1.861	–0.494		
2H-5, 65-67	10.12	84.24	2.059	–0.426	3.382	–1.144
2H-5, 75-77	10.22	85.80	2.201	–0.638	3.691	–1.155
2H-5, 85-87	10.32	87.36	2.291	–0.418	3.675	–1.029
2H-5, 95-97	10.42	88.92			3.703	–0.949
2H-5, 105-107	10.52	90.48			3.666	–1.136
2H-5, 115-117	10.62	91.56			3.670	–0.947
2H-5, 120-122	10.67	92.00	1.580	–0.617		
2H-5, 125-127	10.72	92.44	1.749	–0.377	3.601	–1.101
2H-5, 130-132	10.77	92.88	1.635	0.280		
2H-5, 135-137	10.82	93.32	1.548	–0.362	3.625	–0.902
2H-5, 140-142	10.87	93.76	1.762	–0.320		
2H-5, 145-147	10.92	94.19	1.467	–0.136	3.612	–1.012
2H-6, 0-2	10.97	94.63	1.589	0.132		
2H-6, 5-7	11.02	95.07	1.706	0.070	3.546	–1.138
2H-6, 10-12	11.07	95.51	1.490	–0.278		
2H-6, 15-17	11.12	95.95	1.592	–0.102	3.493	–1.178
2H-6, 20-22	11.17	96.43	1.246	–0.292		
2H, 6, 24-26	11.22	96.97	1.502	–0.153	3.407	–1.122
2H-6, 30-32	11.27	97.52	1.451	–0.201	3.424	–1.216
2H-6, 40-42	11.37	98.61	1.561	–0.374	3.361	–1.433
2H-6, 50-52	11.47	99.70	1.126	–0.419		
2H-6, 55-57	11.52	100.24	1.188	–0.246	3.380	–1.370
2H-6, 60-62	11.57	100.78	1.154	–0.489		
2H-6, 65-67	11.62	101.33	1.785	–0.637	3.328	–1.476
2H-6, 69-71	11.66	101.77	1.390	–0.253		
2H-6, 75-77	11.72	102.42	1.187	–0.316	3.360	–1.294
167-1014D						
2H-4, 85-87	11.88	104.09	1.560	–0.723	3.339	–1.210
2H-4, 85-87	11.88	105.09			3.343	–1.141
2H-4, 105-107	12.08	106.09	1.967	–0.417	3.597	–1.173
2H-4, 110-112	12.13	106.59	1.925	–0.427		
2H-4, 115-117	12.18	107.09			3.494	–1.095
2H-4, 120-122	12.23	107.59	1.333	–0.264		
2H-4, 125-127	12.28	108.09			3.456	–1.009
2H-4, 135-137	12.38	109.09			3.476	–1.200
2H-4, 145-147	12.48	110.09			3.691	–1.119
2H-5, 5-7	12.58	111.18			3.674	–1.192
2H-5, 15-17	12.68	112.49			3.616	–1.161
2H-5, 25-27	12.78	113.80			3.664	–1.076
2H-5, 35-37	12.88	115.11			3.621	–1.046
2H-5, 45-47	12.98	116.41			3.529	–1.082
2H-5, 55-57	13.08	117.72			3.466	–1.120
2H-5, 65-67	13.18	119.03			3.142	–1.244
2H-5, 75-77	13.28	120.34			2.841	–1.140
2H-5, 80-82	13.33	120.99	1.495	–0.657		
2H-5, 85-87	13.38	121.64	1.582	–0.809	2.898	–1.241
2H-5, 90-92	13.43	122.30	1.597	–0.909		
2H-5, 95-97	13.48	122.69	0.529	–1.015	2.785	–1.310
2H-5, 100-102	13.53	122.90	1.523	–0.898		
2H-5, 105-107	13.58	123.11	1.283	–0.977	2.780	–1.403
2H-5, 110-112	13.63	123.32	0.770	–1.088		
2H-5, 115-117	13.68	123.53	0.786	–1.133	2.761	–1.421
2H-5, 120-122	13.73	123.74	1.078	–1.070		
2H-5, 125-127	13.78	123.96	0.280	–1.258	2.822	–1.409
2H-5, 130-132	13.83	124.19	0.512	–1.203		
2H-5, 135-137	13.88	124.41	0.497	–1.102	2.983	–1.561
2H-5, 140-142	13.93	124.64	0.288	–1.241		
2H-5, 145-147	13.98	124.87	0.817	–0.963	3.052	–1.369
2H-6, 0-2	14.03	125.10	0.970	–0.796		
2H-6, 5-7	14.08	125.54	0.671	–0.993	2.896	–1.386
2H-6, 10-12	14.13	126.12	0.938	–0.952		
2H-6, 15-17	14.18	126.70	0.997	–0.894	3.184	–1.461
2H-6, 20-22	14.23	127.28	0.822	–0.992	3.204	–1.472
3H-1, 85-87	14.46	129.89	1.265	–0.984	3.632	–1.399
3H-1, 90-92	14.51	130.16	1.995	–0.720	3.930	–1.555
3H-1, 100-102	14.61	130.71	1.777	–0.908	4.030	–1.218
3H-1, 110-112	14.71	131.25	2.404	–0.806	4.177	–1.302
3H-1, 120-122	14.81	131.79	2.506	–0.581	4.285	–1.283
3H-1, 130-132	14.91	132.33	2.417	–0.707	4.280	–1.274
3H-1, 140-142	15.01	132.87	1.993	–0.628	4.330	–1.368
3H-2, 0-2	15.11	133.41	2.033	–0.929	4.263	–1.360
3H-2, 10-12	15.21	133.95	1.680	–0.866	4.353	–1.212

Table 1 (continued).

Core, section, interval (cm)	Depth (mcd)	Age (ka)	*G. bulloides* ($\delta^{18}O$)	*G. bulloides* ($\delta^{13}C$)	*Uvigerina* ($\delta^{18}O$)	*Uvigerina* ($\delta^{13}C$)
3H-2, 20-22	15.31	134.49	1.816	–0.825	4.350	–1.256
3H-2, 30-32	15.41	135.03	2.464	–0.589	4.316	–1.319
3H-2, 40-42	15.51	135.57	2.189	–0.546	4.345	–1.414
3H-2, 50-52	15.61	136.11	2.585	–0.348	4.281	–1.214
3H-2, 60-62	15.71	136.65	1.963	–0.808	4.277	–1.190
3H-2, 70-72	15.81	137.20	2.201	–0.628	4.218	–1.516
3H-2, 80-82	15.91	137.74	2.422	–0.586	4.382	–1.217
3H-2, 90-92	16.01	138.28	2.383	–0.542	4.233	–1.250
3H-2, 100-102	16.11	138.82	2.382	–0.598	4.188	–1.525
3H-2, 110-112	16.21	139.36	2.387	–0.542	4.214	–1.435
3H-2, 120-122	16.31	139.90	2.083	–0.750	4.151	–1.580
3H-2, 130-132	16.41	140.44	2.517	–0.513	4.151	–1.524
3H-2, 140-142	16.51	140.98	2.670	–0.608	4.113	–1.493
3H-3, 0-2	16.61	141.52	2.443	–0.580	3.995	–1.451
3H-3, 10-12	16.71	142.06	2.879	–0.572	3.918	–1.650
3H-3, 20-22	16.81	143.10	3.006	–0.449	4.187	–1.500
3H-3, 30-32	16.91	144.48	2.773	–0.471	4.164	–1.700
3H-3, 40-42	17.01	145.85	2.757	–0.670	4.145	–1.647
3H-3, 50-52	17.11	147.22	2.292	–0.740	4.054	–1.407
3H-3, 60-62	17.21	148.60	2.804	–0.541	4.203	–1.235
3H-3, 70-72	17.31	149.97	2.437	–0.572	4.267	–1.610
3H-3, 80-82	17.41	151.34	2.428	–0.380	4.155	–1.587
3H-3, 90-92	17.51	143.03	2.058	–0.809	3.934	–1.551
3H-3, 100-102	17.61	144.88	1.891	–0.776	4.028	–1.447
3H-3, 110-112	17.71	146.73	1.915	–0.887	4.028	–1.545
3H-3, 120-122	17.81	148.58	2.472	–0.552	4.057	–1.420
3H-3, 130-132	17.91	150.43	2.434	–0.364	4.078	–1.581
3H-3, 140-142	18.01	152.28	2.011	–0.650	3.304	–1.572
3H-4, 0-2	18.11	154.13	2.223	–0.517	4.100	–1.355
3H-4, 10-12	18.21	155.98	2.188	–0.457	4.090	–1.325
3H-4, 20-22	18.31	157.83	1.907	–0.455	4.134	–1.391
3H-4, 30-32	18.41	159.68	2.050	–0.234	4.065	–1.486
3H-4, 40-42	18.51	161.53	1.937	–0.396	4.056	–1.401
3H-4, 50-52	18.61	163.38	1.930	–0.537	3.891	–1.457
3H-4, 60-62	18.71	165.23	1.797	–0.705	3.821	–1.599
3H-4, 70-72	18.81	167.08	2.266	–0.148	3.864	–1.338
3H-4, 80-82	18.91	168.93	2.407	–0.375	3.807	–1.450
3H-4, 90-92	19.01	170.78	2.173	–0.433	3.878	–1.343
3H-4, 100-102	19.11	172.63	1.743	–0.523	3.825	–1.531
3H-4, 110-112	19.21	174.48	2.125	–0.540	3.760	–1.468
3H-4, 120-122	19.31	176.33	2.080	–0.453	3.840	–1.468
3H-4, 130-132	19.41	178.18	2.392	–0.398	3.891	–1.424
3H-4, 140-142	19.51	187.24	2.210	–0.486	3.862	–1.560

late Quaternary $\delta^{18}O$ deep-sea records from marine isotope Stage (MIS) 6 to the present (Fig. 2). Clearly expressed are the glacial maxima (MISs 6 and 2) represented by the highest $\delta^{18}O$ values (~4.3‰), interglacial MISs 5 and 1 by low $\delta^{18}O$ values (2.6‰ to 3.6‰), and the climate amelioration of MIS 3 and the glacial MIS 4. The last full interglacial marine isotope Substage 5e (Eemian) is clearly recorded as the warmest interval during the last interglacial. The warm Substages 5a and 5c are well pronounced and are separated by the intervening cooler intervals of marine isotope Substages 5b and 5d (Fig. 3). A detailed chronology with at least 20 datums for the last 160 k.y. has been established (Fig. 2) by comparison with a globally averaged record whose fluctuations have been well described (Imbrie et al., 1984; Pisias et al., 1984; Prell et al., 1986) and dated with an average error of ±5 k.y. (Martinson et al., 1987).

Paleoclimatic events at Site 1014 correlated with standard deep-sea oxygen isotope chronology are described in Table 2 (Imbrie et al., 1984). Ages were calculated using linear interpolation between each datum. All stable isotopic values are plotted against kilo years (k.y.) using this standard age model (in standard units of Martinson et al., 1987). Depths of isotopic events identified in this study (Table 2) are graphically correlated (Fig. 3) with the standard deep-sea oxygen isotopic reference section dated by Martinson et al. (1987). In this age vs. depth plot, datums deviate only slightly from a straight line, thus supporting the oxygen isotope stratigraphy for Site 1014. Changes in slope between line segments are interpreted to represent changes in sedimentation rate in the core relative to the reference section. Because these changes in slope are slight, it can be assumed that sedimentation rates were relatively constant. This plot also suggests that there are no significant hiatuses or drilling gaps in the upper 20 mcd at Site 1014. These are predictable results since splicing between the four holes drilled was expected to produce the most complete record at the site. Thus, it is demonstrated that sedimentation rates experienced little change in Tanner Basin during the late Quaternary.

LATE QUATERNARY STABLE OXYGEN ISOTOPE RECORD OF TANNER BASIN

The Site 1014 oxygen isotope record of *G. bulloides* exhibits the familiar climate-related curve for the interval since the penultimate glacial episode (<179 ka) (Fig. 4). Minimum Holocene $\delta^{18}O$ values of ~–0.5‰ are similar to *G. bulloides* $\delta^{18}O$ records in Santa Barbara Basin (Kennett, 1995). After these minimum values, the surface waters of the basin appear to cool as $\delta^{18}O$ values increase (~0.5‰). The maximum $\delta^{18}O$ values of the last glacial maximum recorded in the surface waters of Tanner Basin were ~2.5‰, which were lower than those recorded in Santa Barbara Basin (~3‰). If we assume no change in salinity, the 3‰ shift in $\delta^{18}O$ (–0.5‰–2.5‰) would suggest a ~7°C shift in the temperature of surface waters in Tanner Basin (assuming 1°C is equivalent to 0.23‰ $\delta^{18}O$ [Epstein et al., 1953]). The familiar apparent climate amelioration of MIS 3 can clearly be seen at Site 1014 as well as a concomitant increase in $\delta^{18}O$ variability.

Several differences can be observed between the present interglacial (Holocene) and the last interglacial (MIS 5). The planktonic $\delta^{18}O$ record is incomplete during the last interglacial because of several episodes of dissolution, which resulted in insufficient material for anal-

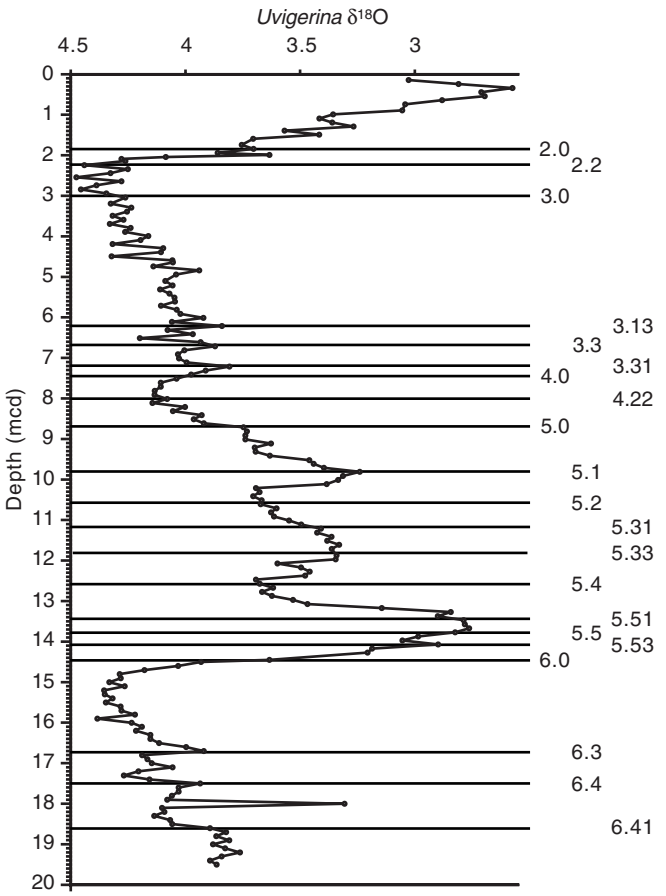

Figure 2. Oxygen isotopic stratigraphy of the benthic foraminifer *Uvigerina* for Site 1014 against depth (in meters composite depth). Oxygen isotopic datums (horizontal lines) are numbered at right, as correlated with the deep-sea oxygen isotopic reference section (Martinson et al., 1987).

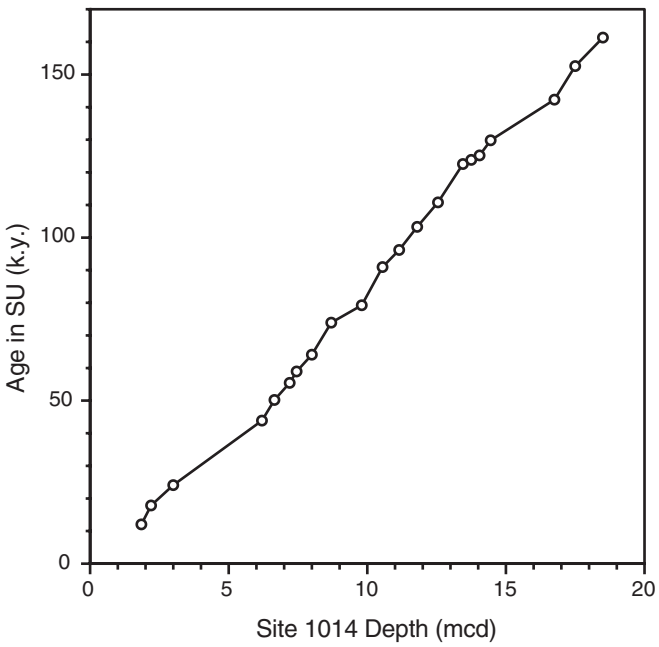

Figure 3. Correlation plot of oxygen isotopic events (datums) recorded at Site 1014 with age in standard units (SU) of the deep-sea oxygen isotopic reference section (Martinson et al., 1987).

Table 2. Depths of oxygen isotopic events (datums) at Site 1014 and their ages in deep-sea standard reference sequence.

Marine isotope substage datum	Depth (mcd)	Age in SU (k.y.)
2	12.05	1.85
2.2	17.85	2.20
3	24.11	3.00
3.13	43.88	6.20
3.3	50.21	6.65
3.31	55.45	7.20
4	58.96	7.45
4.22	64.09	8.00
5	73.91	8.70
5.1	79.25	9.80
5.2	90.95	10.55
5.31	96.21	11.15
5.33	103.29	11.80
5.4	110.79	12.55
5.51	122.56	13.45
5.5	123.82	13.75
5.53	125.19	14.05
6	129.84	14.45
6.3	142.28	16.75
6.4	152.58	17.50
6.41	161.34	18.50

Notes: SU = standard unit (Martinson et al., 1987). Age data are from Martinson et al. (1987).

ysis (Fig. 5). The $\delta^{18}O$ values of this interval are also significantly higher than expected; in particular, the warmest interval of the last interglacial (the Eemian) was 0.8‰ more positive than the Holocene (Fig. 4). Such values, if correct, would indicate that after correcting for ice volume, last interglacial $\delta^{18}O$ values were similar to the glacial, suggesting no change in surface water temperature. It is clear, however, that the Eemian was at least as warm as, if not warmer than, the Holocene (CLIMAP members, 1984; Kennett, 1995). Hence, the Tanner Basin record during this interval was affected by other processes. Our preferred explanation involves the preferential dissolution of thin-shelled specimens, which generally grow at shallower depths and warmer temperatures, biasing the remaining specimens toward higher $\delta^{18}O$ (and thus cooler temperatures). This conjecture is supported by independent methods of estimating SST such as U^{k}_{37}, which suggest that temperatures during marine isotope Substages 5a and 5c were at least as warm as the Holocene and that the Eemian was 3° warmer (Yamamoto et al., 1998). Another explanation involves the increased abundance of the small morphotype of *Gephyrocapsa* species, dominant in upwelling regions during warm interglacial episodes. This suggests that upwelling was more intense during these intervals (Yamamoto et al., 1998). Increased upwelling causing cooler SSTs may not be reflected in the U^{k}_{37} temperatures since it has been shown that U^{k}_{37} values also vary with nutrient availability (Epstein et al., 1998). The strongest evidence against the lowering of sea-surface temperatures by upwelling is the lack of evidence for cool sea-surface temperatures at other sites in the region during this time interval.

Changes in planktonic foraminiferal $\delta^{18}O$ at Site 1014 indicate large SST shifts (~7°C) between the last glacial maximum (MIS 2) and the Holocene (MIS 1). Such large shifts are suggested by earlier $\delta^{18}O$ investigations of the late Quaternary in Tanner Basin, although they were of much lower resolution. Mortyn et al. (1996) found Holocene $\delta^{18}O$ values of ~0.5‰ to –0.5‰ and glacial maximum $\delta^{18}O$ values close to 2.5‰ of *G. bulloides.* Based on these differences and planktonic foraminiferal assemblages (modern analog technique-derived temperatures), it was theorized that SSTs in Southern California were 7° to 8°C cooler during the last glacial maximum (MIS

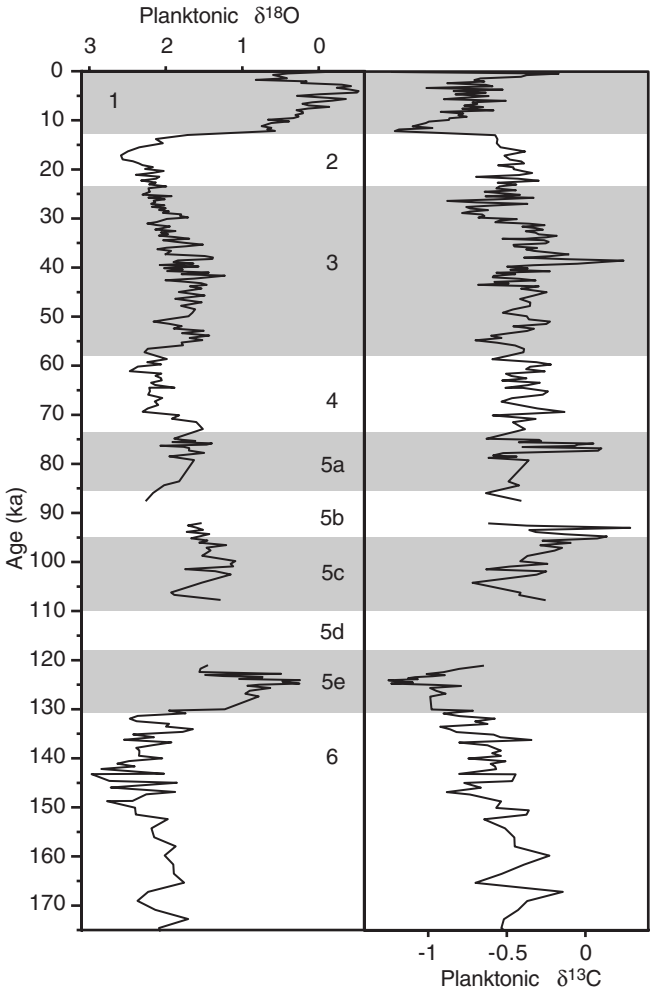

Figure 4. Oxygen and carbon isotopic record for the planktonic foraminifer *Globigerina bulloides* at Site 1014 plotted against age. Oxygen isotopic stages and substages are numbered in the middle; warm intervals are shaded gray.

2). In contrast, Kahn et al. (1981) suggested slightly less glacial–interglacial SST change of ~5°C based on a $\delta^{18}O$ shift from Holocene values of ~0.5‰ and last glacial maximum values of ~2.0‰ in the planktonic foraminifer *Globigerina quinqueloba.* Temperature estimates based on organic geochemical signals (U^{k}_{37}) produced from Site 1014 also suggest an ~5° temperature change between MIS 3 and the Holocene (Yamamoto et al., 1998).

Although changes in the benthic $\delta^{18}O$ record are similar to those of the glacial deep-sea average (Martinson et al., 1987), the differences appear important. During Termination I, the total shift in $\delta^{18}O$ between the glacial maximum and the Holocene is ~2‰ (Fig. 6). It is now well established that changes in oceanic $\delta^{18}O$ composition during this interval were ~1.1‰ because of deglaciation of the Earth's cyrosphere (Shackleton and Opdyke, 1976). Thus, 0.9‰ of the shift in benthic $\delta^{18}O$ must have resulted from temperature and salinity change. Assuming no salinity change and that 1°C is equivalent to 0.23‰ (Epstein et al., 1953), a temperature change of ~4°C would be indicated. Such a large temperature variation would imply a significant shift in the source of intermediate waters in the North Pacific as previously suggested (Kennett and Ingram, 1995; Behl and Kennett, 1996). However, this intermediate water temperature change in the Tanner Basin (~1165 m in depth) appears to be too large since modern bottom temperatures are already at ~3.8°C (Emery, 1954). Near-freezing waters would have resulted, which is unlikely in a shallow water mass at middle latitudes. Clearly, a salinity change must also have contributed to the benthic $\delta^{18}O$ shift at Site 1014. As a 1‰ salinity shift is equivalent to 0.5‰ $\delta^{18}O$ (Craig and Gordon, 1965), it is possible that a significant salinity increase accompanied a cooler intermediate water source. Bottom temperatures could have been ~2°C because glacial North Pacific Intermediate Water may have had a higher component of Pacific Arctic water during the last glacial maximum (Keigwin, 1998). A more reasonable 2°C decrease in temperature would leave 0.45‰ of the $\delta^{18}O$ to be accounted for by a salinity increase of ~0.9‰.

The benthic oxygen isotope record also suggests that there are some differences in the response of benthic $\delta^{18}O$ to global warming during the Eemian and the Holocene. In particular, the early Holocene $\delta^{18}O$ values are ~0.2‰ lower than Eemian values (Fig. 6), implying that bottom waters were warmer or less saline during the early Holocene than during the last interglacial. Furthermore, the duration of the benthic $\delta^{18}O$ decrease at Termination I was much longer (~10 k.y.) than during Termination II (~5 k.y.) (Fig. 6).

LATE QUATERNARY CARBON ISOTOPE RECORD OF TANNER BASIN

A number of trends are shown in the planktonic $\delta^{13}C$ record at Site 1014 (Fig. 4). The most negative values (~1.2‰) recorded in the basin occur during the warmest intervals of the interglacials (marine isotope Substage 5e and the Holocene). During much of the last glacial, the planktonic $\delta^{13}C$ record ranges from ~–0.5‰ to ~–0.25‰ but was interrupted by several positive events (~0.1‰). A number of observations can be made about the Site 1014 *G. bulloides* record compared to other sites on the southern California margin. In Tanner Basin, Holocene $\delta^{13}C$ values (~–0.7‰) and those of the last glacial (~–0.5‰; Fig. 4) are similar to those for Santa Barbara Basin but slightly higher than values from Site 1017. A sharp $\delta^{13}C$ (~0.5‰) decrease occurred during Termination I (Fig. 4), similar to Santa Barbara Basin and Hole 1017E records over the same interval. Another negative $\delta^{13}C$ event lasting ~5 k.y. occurs between 30 and 25 ka and is also found at all three sites (Holes 893A and 1017E; Site 1014).

Thus, it would appear that several regional $\delta^{13}C$ excursions occurred on the southern California margin. Because these events are not reflected in records of *N. pachyderma* $\delta^{13}C$ from Sites 1017 and 893, *G. bulloides* apparently responded to a species-specific forcing, which may be related to changes in nutrient supply of surface waters or surface-water hydrology. Studies have shown that *G. bulloides* calcifies in disequilibria with $\delta^{13}C$ by –2‰ to –4‰, suggesting significant incorporation of metabolic CO_2 into the test during calcification (Sautter and Thunell, 1991). Thus, environmental information retrieved from the *G. bulloides* $\delta^{13}C$ record is limited. However, some evidence shows $\delta^{13}C$ becomes enriched in response to upwelling, possibly as a result of rapid growth and high metabolic activities influenced by nutrient supply, temperature, and PCO_2 (Sautter and Thunell, 1991; Berger and Vincent, 1986).

The Tanner Basin benthic $\delta^{13}C$ record exhibits a general increase (~–1.75‰ to ~–0.75‰) in $\delta^{13}C$ values during the last 200 k.y. (Fig. 6). On a smaller scale, a strong correlation between the benthic $\delta^{13}C$ record and global climate change is exhibited (Fig. 5) at Site 1014. During the last 85 k.y., benthic $\delta^{13}C$ values were higher by ~0.5‰ during warm intervals (MISs 1 and 3; marine isotope Substage 5a) than cool intervals (MISs 2 and 4) (Fig. 6). The opposite relationship is shown during the last interglacial (MIS 5; 130 to 85 ka). Benthic $\delta^{13}C$ increases to ~–1‰ during the cool intervals (marine isotope Substages 5b and 5d) of the interglacial and decreases to ~–1.5‰ during the warmest episodes (marine isotope Substages 5c and 5e) (Fig. 5). Further evidence for changes in the bottom-water chemistry of the basin during the last interglacial is provided by indications of

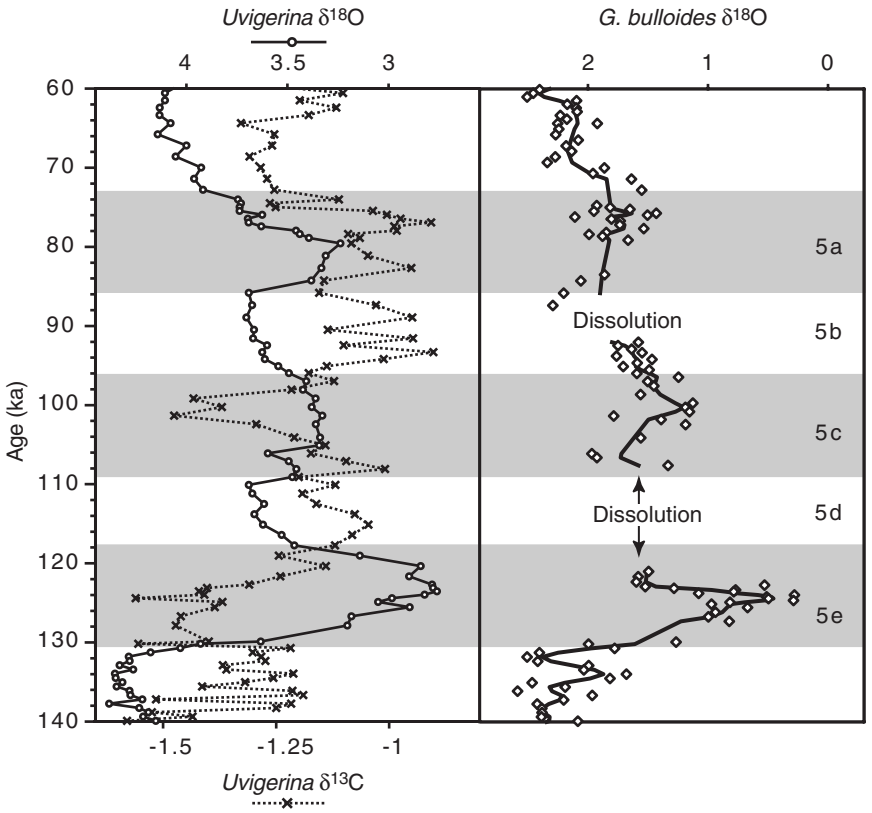

Figure 5. Details of the oxygen and carbon isotopic records of the benthic foraminifer *Uvigerina* spp. and the oxygen isotopic record (smoothed) of the planktonic foraminifer *G. bulloides* for the interval between 140 and 60 ka at Site 1014. On the left, solid line and open circles = $\delta^{18}O$ of *Uvigerina*, dashed line and crosses = $\delta^{13}C$ of the same benthic species. On the right, open diamonds = $\delta^{18}O$ values of the planktonic foraminifer *G. bulloides*, heavy black line = average values. Oxygen isotopic substages are numbered to the right; warm intervals of the last interglacial are shaded gray.

increased corrosivity of the bottom water during the cool episodes (Substages 5b and 5d). Although *Uvigerina* spp. are not considered reliable foraminiferal recorders of deep-water $\delta^{13}C$ because of infaunal habitat, these results suggest that several processes controlled the relative concentrations of ^{12}C.

Benthic $\delta^{13}C$ can be affected by several mechanisms. Globally, the $\delta^{13}C$ reservoir was affected between glacial and interglacial periods by shifts in carbon reservoirs that released more light $\delta^{13}C$ into the ocean, shifts in the $\delta^{13}C$ gradient between oceans, and the effect of lower CO_2 concentration on the carbonate ion (Shackleton and Pisias, 1985). Regionally, the $\delta^{13}C$ value of North Pacific Intermediate Water would have been affected by changes in ventilation, which allowed increased exchange with atmospheric CO_2 during glacial and stadial times (Behl and Kennett, 1996; van Geen et al., 1996). Increased surface ocean CO_2 exchange with the atmosphere would have the effect of enriching $\delta^{13}C$ through processes of both cool-water isotopic equilibrium effects and lower nutrient content as a result of the "newness" of the intermediate water. The length of time a water mass remains isolated from the atmosphere within the deep ocean is related to the quantity of organic material degradation within it, which consumes oxygen and decreases $\delta^{13}C$. Finally, locally within Tanner Basin, interstitial waters were possibly low in $\delta^{13}C$ relative to bottom waters as a result of decay of ^{12}C-enriched organic matter (Berger and Vincent, 1986). Thus, higher organic carbon flux should result in higher $\Delta\delta^{13}C$ between bottom waters and the sediment depth in which *Uvigerina* lived.

Another explanation for the unusual aspects of both the $\delta^{18}O$ and $\delta^{13}C$ records of Tanner Basin might be diagenesis. Diagenesis can play an important role in changing the isotopic composition of biogenic calcium carbonate after burial by encrustation of tests by secondarily precipitated calcite. This can bias isotopic paleotemperatures to cooler values (Douglas and Savin, 1978). The unusually cool last interglacial sea-surface temperatures could perhaps be explained by this process as well as the change in the relationship between benthic $\delta^{13}C$ and climate. However, diagenesis would affect both planktonic and benthic tests so that both records would show similar trends in isotopic behavior and would mask regional similarities between Tanner Basin and other sites along the southern California margin. This is not the case: the $\delta^{13}C$ record during marine isotope Substage 5e in Site 1014 is more similar to that of Holes 893A and 1017E than to the Tanner Basin benthic $\delta^{13}C$ record. Site 1014 benthic $\delta^{18}O$ does not show the unusual cooling suggested by the planktonic record. Finally, such diagenesis is uncommon in the shallow-buried sediments as young as those investigated in this contribution.

LATE QUATERNARY PALEOCEANOGRAPHIC IMPLICATIONS OF THE SITE 1014 RECORD

Late Quaternary Sea-Surface Temperatures in the Southern California Margin

Major changes in the surface waters occurred in the southern California margin in response to late Quaternary climate change (Thunell and Mortyn, 1995; Kennett and Ingram, 1995; Sabin and Pisias, 1996; Prahl et al., 1995), and these changes are reflected at Site 1014 by large $\delta^{18}O$ shifts (Figs. 4, 5). Earlier work has also suggested that low SSTs off the west coast of North America during the last glacial maximum were associated with the increased influence of subarctic waters in the region, resulting in the southward displacement of currents and related atmospheric systems (Thunell and Mortyn, 1995; Sabin and Pisias, 1996; Prahl et al., 1995). Ocean-atmosphere interactions over the North Pacific Ocean determine the strength and location of currents along the California margin (Reid et al., 1958). It is reasonable to conclude that with the atmospheric reorganization accompanying the formation of large ice sheets (COHMAP members, 1988) and cooler high-latitude SSTs, the relationship would have changed between the California Current and countercurrent. Thus, large inferred temperature shifts between glacial and interglacial in surface

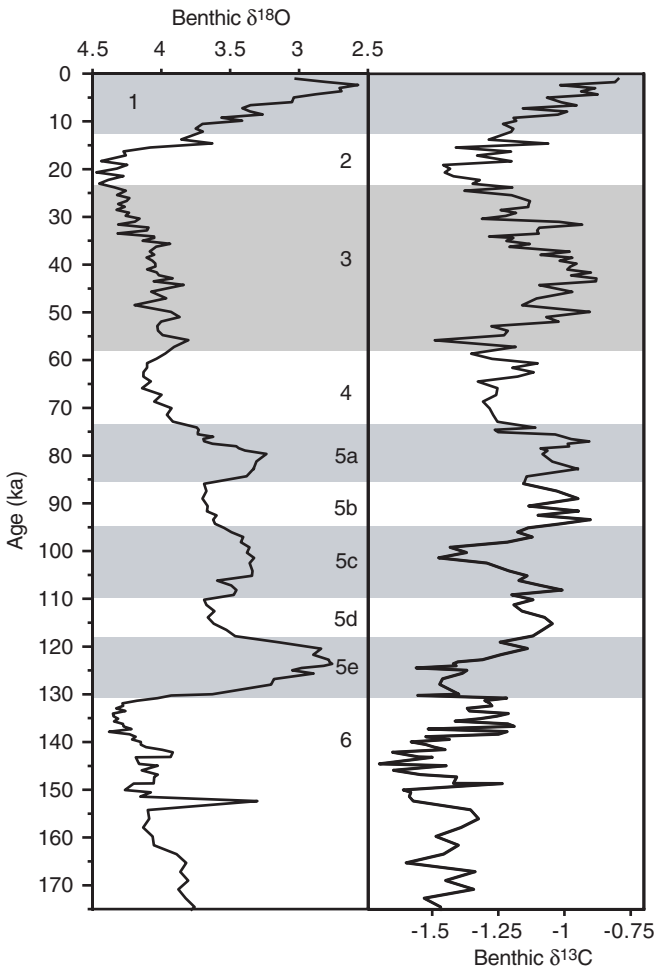

Figure 6. Oxygen and carbon isotopic record for the benthic foraminifer *Uvigerina* at Site 1014 plotted against age. Oxygen isotopic stages are numbered in the middle; warm intervals are shaded in gray.

waters in Tanner Basin probably resulted from changing dominance of a cooler, intensified California Current relative to the warm countercurrent. As well, countercurrent influence at Site 1014 would be negligible, and SSTs would be much reduced if geostrophic flow created by the surface ocean pressure difference between San Diego and Point Conception was not established during glacial times.

Late Quaternary Productivity

Site 1014 lies in the outermost basins of the California Borderland; consequently, lithogenic input is minor from the nearby continent, whereas biogenic deposition makes the largest contribution to the sediment budget of the basin (Gorsline and Teng, 1989). Because changes in biogenic sedimentation can be used to estimate changes in productivity, an almost constant sedimentation rate suggests that the deposition of biogenic material did not significantly differ between glacial and interglacial episodes. However, this simple relationship is complicated by several factors. First, the sedimentation rate reflects averaged biogenic deposition as rates are interpolated between datums, so that short-term events are not discernible. Second, carbonate dissolution reduces sedimentation rates by removing deposited biogenic sediment so that increased productivity may be masked. This particularly complicated the record during the last interglacial when deposition of organic material increased (Yamamoto et al., 1998) during marine isotope Substages 5b and 5d as did the severity of dissolution. Yet sedimentation rates remained generally constant.

The benthic $\delta^{13}C$ record may provide evidence of changes in surface water productivity because the interstitial waters inhabited by the foraminifers are affected by degradation of organic matter. During the cooler substages (5b and 5d) of the last interglacial, organic carbon accumulation increased when benthic $\delta^{13}C$ values were higher. This result is confirmed by the increased accumulation rates of alkenones (Haptophytes), dinosterol (dinoflagellates) and bishomohopanol (bacteria), and higher plant biomarkers that show similar variations to organic carbon (Yamamoto et al., 1998). The relationship is opposite to the one expected if benthic $\delta^{13}C$ were responding to organic material deposition. It appears that there is not a simple relationship between the production of organic material in the surface waters and benthic $\delta^{13}C$. The record during marine isotope Substages 5b and 5d is further complicated by an anticorrelation between organic accumulation rate and upwelling indicators. This suggests that episodes of intensified upwelling are not accompanied by increased organic carbon deposition (Yamamoto et al., 1998).

Attempts at estimating productivity changes on the California Borderland have been published by several authors. Mortyn and Thunell (1997) suggested productivity increases during the last glacial maximum that are 1.5 to 2.0 times greater than the Holocene; they attribute this increase to intensification of the California Current and enhanced upwelling south of 40°N. On the other hand, Berger et al. (1997) observed a significant reduction in opaline deposits in the Santa Barbara Basin, which they attributed to a decrease in estuarine conditions of the North Pacific. It is possible that during glacial episodes, upwelling intensified in the California Current. However, because of the increased contribution of North Pacific sourced Intermediate Water, water being upwelled was nutrient poor, and productivity did not significantly rise. Nevertheless, during interglacials the northern component of Pacific glacial Intermediate Water diminished in relation to old, deep Pacific water. Hence, although upwelling was reduced, surface waters had a higher nutrient content (Behl and Kennett, 1996; van Geen et al., 1996). Thus, complicating factors of both the North Pacific and Tanner Basin prevent support of significant climate-induced changes in productivity during cool intervals.

Late Quaternary Ventilation of Tanner Basin

The relationship between the benthic $\delta^{13}C$ record and ventilation of the North Pacific at Site 1014 is complicated. The record (Fig. 6) does not appear to represent changes in ventilation of the basin during the last 85 k.y. but instead follows the global $\delta^{13}C$ record (Shackleton and Pisias, 1985) with lower values during cool intervals. During the last interglacial (MIS 5), the response of benthic $\delta^{13}C$ changed, no longer conforming to the global pattern. Consequently, changes in $\delta^{13}C$ appear to represent a delicate balance between the dominance of the flux of organic carbon at the site, ventilation of the water mass entering the basin, and global carbon isotope production.

Benthic $\delta^{13}C$ might be responding to the age of the deep water mass and the resulting ventilation as mentioned above, where old, poorly ventilated water typically has lower $\delta^{13}C$ values than newer, well-ventilated water masses. The current paradigm involving North Pacific Intermediate Water suggests that during warmer climates, the water mass becomes increasingly poorly ventilated (Behl and Kennett, 1996; van Geen et al., 1996); thus, $\delta^{13}C$ should be lower. This corresponds to the $\delta^{13}C$ benthic record of Tanner Basin (Fig. 5), where $\delta^{13}C$ decreased during the warm intervals of the last interglacial (marine isotope Substages 5c and 5e). High PCO_2 content—either from old, poorly ventilated water resulting from considerable decomposition of organic material or cool water saturated in CO_2—enhanced corrosivity of a water mass. However, intervals of corrosion,

which punctuate carbonate sedimentation in Tanner Basin during the cool Substages 5b and 5c, are anticorrelated with the ventilation and $\delta^{13}C$ relationship. Therefore, during cool intervals (marine isotope Substages 5b and 5d) of the last interglacial, PCO_2 levels of intermediate waters were not connected to the ventilation history of the water. Consequently, the Tanner Basin record agrees with others from the California margin (Kennett and Ingram, 1995; Behl and Kennett, 1996; van Geen et al., 1996), indicating that ventilation of North Pacific Intermediate Water changed in response to climate change.

CONCLUSIONS

- Stable oxygen isotope records from Site 1014 exhibit the familiar sawtooth pattern of late Quaternary climate change.
- A detailed chronology for the last 175 k.y. has been developed based on 20 stable isotope datums (SPECMAP) for Site 1014.
- There are no major hiatuses in the late Quaternary at Site 1014, and sedimentation rates in the basin were almost constant, with average rates of 11.5 cm $k.y.^{-1}$
- The planktonic foraminiferal $\delta^{18}O$ record shows that the magnitude of the glacial–interglacial temperature change was ~7°C, similar to results from other lower resolution cores from Tanner Basin, and agrees with other southern California margin cores.
- During the last interglacial, the planktonic $\delta^{18}O$ record was affected by several episodes of dissolution that coincided with cooler marine isotope Substages 5b and 5d.
- Last interglacial planktonic $\delta^{18}O$ values were higher than Holocene values by more than 0.8‰, apparently not because of cooler temperatures but as a result of the effects of preferential dissolution of thin-shelled specimens.
- The glacial–interglacial change in benthic $\delta^{18}O$ was unusually large for a water depth of 1165 m, suggesting that both temperature and salinity changed dramatically over this interval in response to switches in the source of the intermediate water mass bathing the site.
- Planktonic $\delta^{13}C$ values are similar to other southern California sequences and display similar negative excursions during Termination I and late MIS 3. This suggests that these events were regional.
- The benthic $\delta^{13}C$ record correlated well with the global $\delta^{13}C$ record during the last 85 k.y., suggesting that ventilation and productivity effects at this location and depth were minor over this interval.
- Between 135 and 85 ka, the benthic $\delta^{13}C$ record was controlled by ventilation of the intermediate water and was linked to changes in upwelling, organic material deposition, and corrosivity of the bottom water.
- The benthic $\delta^{18}O$ Holocene record differs from the Eemian by exhibiting a slow decrease in $\delta^{18}O$ during Termination I, leading to lighter values than the previous interglacial.

ACKNOWLEDGMENTS

We thank Karen Thompson and Howard Berg for their valuable technical support. This research was supported by JOI/USSAC post-cruise funding (ODP Leg 167) and the National Science Foundation (Earth System History). I. Hendy has been supported by a National Science Foundation Coastal Research Fellowship. We thank D. Kroon, M. Maslin, and M. Lyle for their useful suggestions toward the improvement of this contribution.

REFERENCES

Behl, R.J., and Kennett, J.P., 1996. Evidence for brief interstadial events in the Santa Barbara Basin, NE Pacific during the past 60 Kyr. *Nature,* 379:243–246.

Berger, W., Lange, C., and Weinheimer, A., 1997. Silica depletion of the thermocline in the eastern North Pacific during glacial conditions: clues from Ocean Drilling Program Site 893, Santa Barbara Basin, California. *Geology,* 25: 619–622.

Berger, W.H., and Vincent, E., 1986. Deep-sea carbonates: reading the carbon-isotope signal. *Geol. Rundsch.,* 75:249–269.

CLIMAP Project Members, 1984. The last interglacial ocean. *Quat. Res.,* 21:123–224.

COHMAP Members, 1988. Climatic changes of the last 18,000 years: observations and model simulations. *Science,* 241:1043–1052.

Coplen, T.B., 1996. Editorial: more uncertainty than necessary. *Paleoceanography,* 11:369–370.

Craig, H., and Gordon, L.I., 1965. Deuterium and oxygen-18 variations in the ocean and the marine atmosphere. *In* Tongiorgi, E. (Ed.), *Stable Isotopes in Oceanographic Studies and Paleotemperatures:* Pisa (Cons. Naz. delle Ric., Lab. di Geol. Nucleare), 9–130.

Douglas, R.G., and Savin, S.M., 1978. Oxygen isotopic evidence for the depth stratification of Tertiary and Cretaceous planktic Foraminifera. *Mar. Micropaleontol.,* 3:175–196.

Emery, K.O., 1954. Source of water in basins off southern California. *J. Mar. Res.,* 13:1–21.

————, 1960. *The Sea Off Southern California: A Modern Habitat of Petroleum:* New York (Wiley).

Epstein, B., D'Hondt, S., Quinn, J., and Zhang, J., 1998. An effect of dissolved nutrient concentrations on alkenone-based temperature estimates. *Paleoceanography,* 13:122–126.

Epstein, S., Buchsbaum, S.R., Lowenstein, H.A., and Urey, H.C., 1953. Revised carbonate-water isotopic temperature scale. *Geol. Soc. Am. Bull.,* 64:1315–1326.

Gorsline, D.S., and Teng, L.S.-Y., 1989. The California Continental Borderland. *In* Winterer, E.L., Hussong, D.M., and Decker, R.W. (Eds.), *The Geology of North America* (Vol. N): *The Eastern Pacific Ocean and Hawaii.* Geol. Soc. Am., 471–487.

Imbrie, J., Hays, J.D., Martinson, D.G., McIntyre, A., Mix, A.C., Morley, J.J., Pisias, N.G., Prell, W.L., and Shackleton, N.J., 1984. The orbital theory of Pleistocene climate: support from a revised chronology of the marine $\delta^{18}O$ record. *In* Berger, A., Imbrie, J., Hays, J., Kukla, G., and Saltzman, B. (Eds.), *Milankovitch and Climate* (Pt. 1), NATO ASI Ser. C, Math Phys. Sci., 126:269–305.

Kahn, M.I., Oba, T., and Ku, T.-L., 1981. Paleotemperatures and glacially induced changes in the oxygen-isotope composition of seawater during the late Pleistocene and Holocene time in Tanner Basin, California. *Geology,* 9:485–490.

Keigwin, L.D., 1998. Glacial-age hydrology of the far northwest Pacific. *Paleoceanography,* 13:323–339.

Kennett, J.P., 1995. Latest Quaternary benthic oxygen and carbon isotope stratigraphy: Hole 893A, Santa Barbara Basin, California. *In* Kennett, J.P., Baldauf, J.G., and Lyle, M. (Eds.), *Proc. ODP, Sci. Results,* 146 (Pt. 2): College Station, TX (Ocean Drilling Program), 3–18.

Kennett, J.P., and Ingram, B.L., 1995. A 20,000-year record of ocean circulation and climate change from the Santa Barbara Basin. *Nature,* 377:510–512.

Lyle, M., Koizumi, I., Richter, C., et al., 1997. *Proc. ODP, Init. Repts.,* 167: College Station, TX (Ocean Drilling Program).

Lynn, R.J., and Simpson, J.J., 1987. The California Current system: the seasonal variability of its physical characteristics. *J. Geophys. Res.,* 92:12947–12966.

Martinson, D.G., Pisias, N.G., Hays, J.D., Imbrie, J., Moore, T.C., Jr., and Shackleton, N.J., 1987. Age dating and the orbital theory of the ice ages: development of a high-resolution 0 to 300,000-year chronostratigraphy. *Quat. Res.,* 27:1–29.

Mortyn, P., Thunell, R., Anderson, D., Stott, L., and Le, J., 1996. Sea surface temperature changes in the Southern California Borderlands during the last glacial-interglacial cycle. *Paleoceanography,* 11:415–430.

Mortyn, P.G., and Thunell, R.C., 1997. Biogenic sedimentation and surface productivity changes in the Southern California Borderlands during the last glacial-interglacial cycle. *Mar. Geol.,* 138:171–192.

Pak, D., and Kennett, J.P., 1997. Planktonic foraminiferal proxies of hydrographic conditions in the Santa Barbara Basin. *Fall Am. Geophys. Union,* 78.

Pisias, N.G., 1978. Paleoceanography of the Santa Barbara Basin during the last 8000 years. *Quat. Res.,* 10:366–384.

Pisias, N.G., Martinson, D.G., Moore, T.C., Shackleton, N.J., Prell, W., Hays, J., and Boden, G., 1984. High resolution stratigraphic correlation of benthic oxygen isotopic records spanning the last 300,000 years. *Mar. Geol.,* 56:119–136.

Prahl, F.G., Pisias, N., Sparrow, M.A., and Sabin, A., 1995. Assessment of sea-surface temperature at 42° N in the California Current over the last 30,000 years. *Paleoceanography,* 10:763–773.

Prell, W.L., Imbrie, J., Martinson, D.G., Morley, J.J., Pisias, N.G., Shackleton, N.J., and Streeter, H.F., 1986. Graphic correlation of oxygen isotope stratigraphy: application to the late Quaternary. *Paleoceanography,* 1:137–162.

Reid, J.L., Jr., Roden, G.I., and Wyllie, J.G., 1958. Studies of the California Current system. *Calif. Coop. Oceanic Fisheries Invest. Rep.,* 6:27–56.

Sabin, A.L., and Pisias, N.G., 1996. Sea Surface temperature changes in the Northeastern Pacific Ocean during the past 20,000 years and their relationship to climate change in Northwestern North America. *Quat. Res.,* 46:48–61.

Sautter, L.R., and Thunell, R.C., 1991. Seasonal variability in the $\delta^{18}O$ and $\delta^{13}C$ of planktonic foraminifera from an upwelling environment: sediment trap results from the San Pedro Basin, Southern California Bight. *Paleoceanography,* 6:307–334.

Shackleton, N.J., 1974. Attainment of isotopic equilibrium between ocean water and benthonic foraminifera genus *Uvigerina:* isotopic changes in the ocean during the last glacial. *Cent. Nat. Res., Sci. Colloq. Int.,* 219: 203–209.

Shackleton, N.J., and Opdyke, N.D., 1976. Oxygen isotope and paleomagnetic stratigraphy of equatorial Pacific core V28-238: oxygen isotope temperatures and ice volumes on a 10^5 year and 10^6 year scale. *Quat. Res.,* 3:39–55.

Shackleton, N.J., and Pisias, N.G., 1985. Atmospheric carbon dioxide, orbital forcing, and climate. *In* Sundquist, E.T., and Broecker, W.S. (Eds.), *The Carbon Cycle and Atmospheric CO_2: Natural Variations Archean to Present.* Geophys. Monogr., Am. Geophys. Union, 32:303–317.

Thunell, R.C., and Mortyn, P.G., 1995. Glacial climate instability in the Northeast Pacific Ocean. *Nature,* 376:504–506.

Thunell, R.C., and Sautter, L.R., 1992. Planktonic foraminiferal faunal and stable isotopic indices of upwelling: a sediment trap study in the San Pedro Basin, Southern California Bight. *In* Summerhayes, C.P., Prell, W.L., and Emeis, K.C. (Eds.), *Upwelling Systems: Evolution Since the Early Miocene.* Geol. Soc. Spec. Publ. London, 64: 77–91.

van Geen, A., Fairbanks, R.G., Dartnell, P., McGann, M., Gardner, J.V., and Kashgarian, M., 1996. Ventilation changes in the northeast Pacific during the last deglaciation. *Paleoceanography,* 11:519–528.

Winant, C.D., and Dorman, C.E., 1997. Seasonal patterns of surface wind stress and heat flux over the Southern California Bight. *J. Geophys. Res.,* 102:5641–5653.

Yamamoto, M., Tanaka, Y., Yamamuro, M., Hendy, I., and Kennett, J., 1998. Organic geochemical and nannofossil records from Site 1014, Tanner Basin during the last 170,000 years. *Spring Am. Geophys. Union,* 79.

Date of initial receipt: 2 November 1998
Date of acceptance: 19 April 1999
Ms 167SR-205